Effects of Protonation on the Spectroscopic Properties of Tetrapyridoacridine (TPAC) Mono- and Dinuclear Ru(II) Complexes in Their Ground and [3]MLCT Excited States

Leslie Herman, Benjamin Elias, Frédéric Pierard, Cécile Moucheron, and Andrée Kirsch-De Mesmaeker*

Service de Chimie Organique et Photochimie, CP 160/08, Université libre de Bruxelles, 50 Avenue F.D. Roosevelt, B-1050 Bruxelles, Belgium

The spectroscopic behavior of mono- and dinuclear Ru(II) complexes (**P, T, PP** and **TT,** Figure 1) that contain the extended planar ligand tetrapyrido[3,2-a:2′,3′-c:3″,2″-h:2‴,3‴-j]acridine (TPAC) and either 1,-10-phenanthroline (phen) or 1,4,5,8-tetraazaphenanthrene (tap) as ancillary ligands is examined in water and as a function of the pH. These four complexes luminesce in aqueous solution. The analyses of the data in absorption lead to the pK_a values in the ground state, and the data in emission show that the excited [3]MLCT states are much more basic than the ground state. When the complex contains tap ligands (**T** and **TT**), a decrease in pH transforms the luminescent excited basic form into another luminescent excited protonated species, which emits more bathochromically. In contrast, with phen ancillary ligands (**P** and **PP**), the protonated excited state does not luminesce. The rate constant of first protonation of the [3]MLCT state is diffusion controlled, except for the dinuclear **PP** complex, whose protonation takes place on the nitrogen of the acridine motif. For **P,** in which the protonation process is the fastest, it would take place on the nitrogen atoms of the nonchelated phen moiety of the TPAC ligand. These results allow also us to gain information on the localization of the excited electron in the [1]MLCT state populated upon absorption as well as in the relaxed [3]MLCT emissive state. Moreover as these complexes are interesting for their study with DNA, it can be concluded from these data that a portion of the excited species in interaction with DNA will be protonated.

Introduction

For the last several years, many research teams and our own group have examined the excited-state properties of polyazaaromatic Ru(II) complexes in the presence of mononucleotides,[1,2] polynucleotides, DNA,[3–8] and amino acids.[9–13] We have shown that when the complex contains at least two tap ligands (tap = 1,4,5,8-tetraazaphenanthrene) and is in presence of DNA[14–16] or some amino acids,[17,18] an electron transfer takes place from a guanine or a tryptophane unit to the excited complex. This photoinduced charge-transfer reaction is related to the high oxidation power of these complexes in their excited state.

To gain insight into the mechanisms of deactivation of the excited states of these photoreactive or photoluminescent complexes in the presence of these different biological reagents, one has to carry out laser flash photolysis studies including kinetic analyses in different timescales (microseconds to 100 fs).[19–21] As biomolecules are involved in these studies, aqueous solutions have to be used and consequently, even if the photophysics has been studied in organic solvents, the photochemical or photophysical mechanisms must also be determined in water. Therefore, the question that is often raised for the interpretation of the transient absorption spectra and the kinetics in these time domains in aqueous solutions is whether the excited states can be protonated in the chosen experimental conditions. The numerous publications concerning the behavior of the well-known [Ru(bpy/phen)$_2$dppz]$^{2+}$ complex[22–24] (bpy = 2,2′-bipyridine, phen = 1,10-phenanthroline, dppz = dipyrido[3,2-a:2′,3′-c]phenazine) in water in the absence or presence

of DNA, and where the possibility of protonation was discussed,[25–27] illustrate the fact that the pK_a values are important parameters to be considered.

Recently, we have prepared and characterized mono- and dinuclear TPAC (TPAC = tetrapyrido[3,2-a:2′,3′-c:3″,2″-h:2‴,3‴-j]acridine) complexes with phen or tap (tap = 1,4,5,8-tetraazaphenanthrene) as ancillary ligands (Figure 1).[28] Although their behaviors have been examined in acetonitrile,[28] it is important to determine the properties of the ground and excited state of these complexes in water for different pH values for the above-mentioned reasons. This study is particularly important for the complexes of Figure 1, which contain different heterocyclic nitrogens susceptible to protonation (the tap and TPAC nitrogens) and which should very well interact and photoreact with DNA. Moreover, because the pK_a data constitute a prerequisite for reliable analyses of the short-lived transients produced under pulsed laser excitation in the absence and presence of DNA, we have examined in this work the effect of pH on the four TPAC complexes of Figure 1 and determined the pK_a values in the ground and excited state.

Experimental Section

Syntheses. The syntheses and purifications of the four TPAC complexes of Figure 1 have been described elsewhere.[28]

Chemicals. Spectroscopic grade acetonitrile from Fluka was used for the photophysical measurements. Acidity of the solutions in the 0–14 pH range was adjusted by adding HCl for analysis (Ridel-De Haën), and the pH measurements were performed using a 3 mm glass microelectrode (Fisher Bioblock Scientific) and a P601 Consort pH meter, with standard buffers

* Corresponding author. E-mail: akirsch@ulb.ac.be.
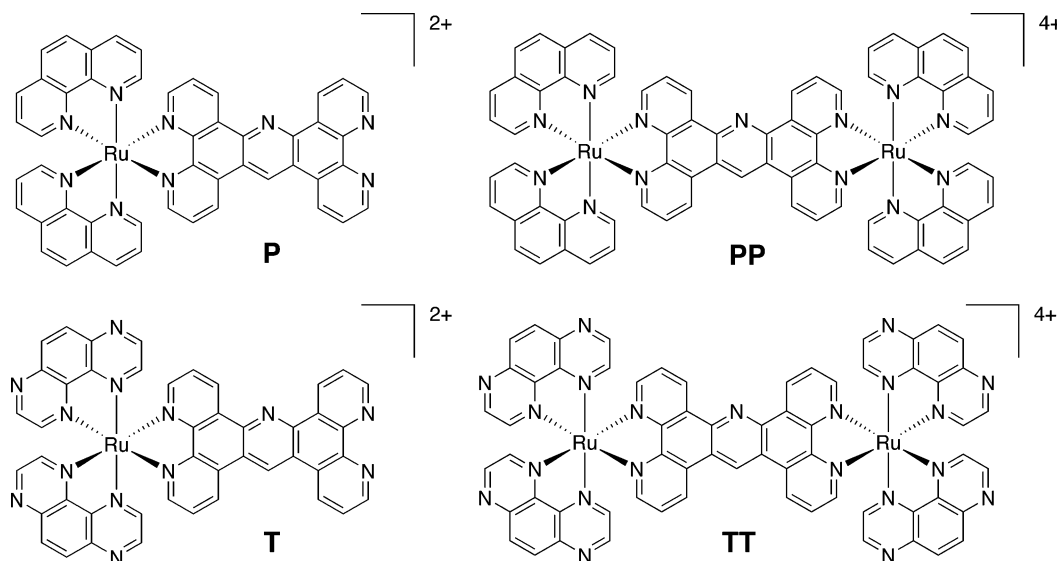
Figure 1. TPAC complexes: [Ru (phen)$_2$TPAC]$^{2+}$ **P**, [(phen)$_2$ Ru TPAC Ru (phen)$_2$]$^{4+}$ **PP**, [Ru (tap)$_2$TPAC]$^{2+}$ **T**, and [(tap)$_2$ Ru TPAC Ru (tap)$_2$]$^{4+}$ **TT**; phen = 1,10-phenanthroline, TPAC = tetrapyrido[3,2-a:2′,3′-c:3″,2″-h:2‴,3‴-j]acridine, and tap = 1,4,5,8-tetraazaphenanthrene.

TABLE 1: Absorption and Emission Data in H$_2$O at 298K for the Complexes P, PP, T, TT,^{a} and Some Reference Complexes

	absorbance λ_{max}^{abs}, nm ($\epsilon \times 10^3$ M^{-1}cm^{-1})		emission^b		
	UV	visible	λ_{max}^{em} (nm)	$\tau^{air(Ar)}$ (ns)	$\phi^{air(Ar)} \times 10^{-3}$
P	263, 281, 321^{sh}	420^{sh}, 450 (19.9)	613	500 (839)	71 (99)
PP	263, 279^{sh}, 320^{sh}, 355	420^{sh}, 450 (39.2)	614	491 (855)	60 (98)
[Ru (phen)$_3$]$^{2+c,d}$	202, 224, 262	421, 447 (19.0)	604	480 (990)	(57)
T	232, 280, 318^{sh}	413 (19.3), 462^{sh}	640	759 (952)	20 (23)
TT	278, 316^{sh}	416 (35.9), 465^{sh}	640	739 (919)	25 (31)
[Ru (tap)$_2$phen]$^{2+e}$	202, 230, 272	410, 465 (14.5)	642	690 (835)	25

^{a} Measurements with solutions 1×10^{-5} mol dm^{-3} in complex in aerated solution. The lifetimes and the quantum yields are given under air and under Ar. ^{b} Corrected for the instrument response. ^{c} See ref 29. ^{d} See ref 30. ^{e} See ref 31. sh = shoulder.

for the calibration of the electrode. To reach higher acidity ranges, sulfuric acid for analysis (Ridel-De Haën) was added to the complex solutions. All the experiments were performed with Millipore Milli-Q purified water. The experiments under Ar were carried out after extensive deoxygenation with Ar of high purity.

Instrumentation. The absorption spectra were recorded on a Perkin-Elmer Lambda 40 UV/vis spectrophotometer.The emission spectra in the 500−800 nm range were recorded with a Shimadzu RF-5001 PC spectrofluorimeter with a 250 W Xe Lamp as exciting source and a Hamamatsu R-928 red-sensitive photomultiplier tube for detection. For the four TPAC complexes, no shift in λ_{max} of luminescence was observed as a function of the pH. For emissions at $\lambda > 800$ nm, the spectra were recorded with an Edinburgh Instruments FS-900 steady-state T-geometry fluorimeter (Edinburgh Instruments, U.K.) with a 450 W Xe Lamp exciting source and an infrared Ge-detector North Coast EO 817L equipped with a muon filter (Edinburgh Instruments, U.K.) and cooled with liquid nitrogen. All the emission spectra were corrected for the response of the detector.

Quantum yields of emission were measured in comparison with the quantum yield of the reference complex [Ru (bpy)$_3$]$^{2+}$ (0.028 in water under air)[29] by adjusting the optical density at the wavelength of excitation (450 nm) at the same percentage of absorbed light. The luminescence lifetimes were measured by using the time-correlated single photon counting technique (TCSPC) with an Edinburgh Instruments FL-900 spectrometer equipped with a nitrogen-filled discharge lamp and a Peltier-cooled Hamamatsu R955s photomultiplier tube. The emission decays were analyzed with the Edinburgh Instruments software

(version 3.0) on the basis of nonlinear least-squares regressions using Marquardt algorithms.

Luminescence lifetimes as a function of pH for the Stern−Volmer plots were measured with a modified Applied Photophysics laser kinetic spectrometer ($\tau_{pulse} \sim 8$ ns) by exciting the samples with a frequency doubled Nd:YAG pulsed laser at 355 nm (Continuum NY 61−10) with a power of 8 mJ/pulse. The emission decays were detected with a R-928 Hamamatsu photomultiplier tube whose output was applied to a digital oscilloscope (Hewlett-Packard HP 54200A) interfaced to a Hewlett-Packard HP 9816 S computer. Signals were averaged over 16 shots.

Results and Discussion

Spectroscopic Properties in Water. The spectroscopic data in absorption and emission for aqueous solutions of mono- and dinuclear TPAC complexes in the absence of acid, base, or buffer are gathered in Table 1 along with those of some reference complexes for comparison. On the basis of these data, the four complexes of Figure 1 can be divided into two categories: (i) the complexes bearing phen ancillary ligands, thus the mononuclear [Ru (phen)$_2$TPAC]$^{2+}$ **P** and the dinuclear [(phen)$_2$ Ru TPAC Ru (phen)$_2$]$^{4+}$ **PP**, and (ii) the coumpounds containing tap ancillary ligands, thus the mononuclear [Ru (tap)$_2$TPAC]$^{2+}$ **T** and the dinuclear [(tap)$_2$ Ru TPAC Ru (tap)$_2$]$^{4+}$ **TT**.

For the phen complexes (**P** and **PP**), the λ_{max} of absorption and emission in water are comparable to those of [Ru (phen)$_3$]$^{2+}$.[29,30] The ^{1}MLCT (metal to ligand charge transfer) excited-state populated by absorption corresponds in this case
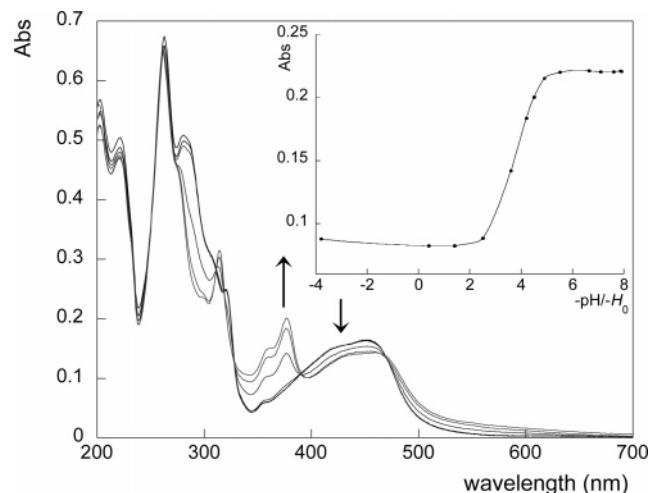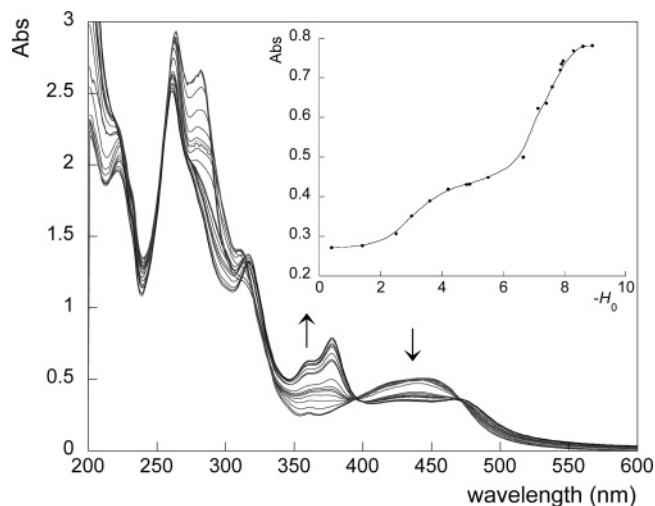
Figure 2. Absorption spectra of [(phen)$_2$ Ru TPAC Ru (phen)$_2$]$^{4+}$ (**PP**) for increasing protonating powers (represented: pH 3.8, $H_0 = -0.4$, -1.4, -2.5, -3.6, -4.2, -4.9). Inset: spectrophotometric titration curve at 376 nm corresponding to the protonation of the acridine moiety of the TPAC bridging ligand from which the K_{a1} value is retrieved.

Figure 3. Absorption spectra of [Ru (phen)$_2$TPAC]$^{2+}$ (**P**) for increasing powers of protonation (represented for $H_0 = -0.4$, -1.4, -2.5, -3.6, -4.2, -4.9, -5.5, -6.6, -7.1, -7.6, -7.8, -7.9). Inset: spectrophotometric titration curve at 376 nm with two inflection points corresponding to the values of pK_{a1} and pK_{a2}.

to a charge transfer to the TPAC ligand, concluded from the reduction potential data in MeCN.[28] For the tap complexes (**T** and **TT**), again on the basis of the electrochemical data in MeCN,[28] the most bathochromic transition corresponds to a CT process in which the electron is transferred to one of the π-deficient tap ligands. This is also in agreement with the similarity of the λ_{max} of absorption and emission between **T**, **TT**, and [Ru (tap)$_2$phen]$^{2+}$.[31]

Moreover, the luminescence quantum yields for the TPAC complexes show that the phen-containing compounds have the same ϕ_{em} under argon ($\sim$0.1), whereas all the tap-containing complexes have a lower quantum yield of emission. These data indicate that the luminophore for **P** and **PP** (MLCT Ru-TPAC) is not the same as that for **T** and **TT** (MLCT Ru-tap). On the other hand, it may also be concluded from Table 1 that the characteristics of the TPAC complexes are not much affected by the dinucleation. This is expected for the **TT** complex, because the ^{3}MLCT Ru-tap excited state is involved in the emission and not the ^{3}MLCT Ru-TPAC state. For the **P** complex, studies with MeCN solutions as a function of temperature suggested that **P** has two Ru-TPAC emitting states[28] whose relative population depends on the temperature, which is not the case for the **PP** complex. These studies also showed that the dinuclear compounds behave quasi as twice the mononuclear TPAC complexes; thus this is in agreement with the molar absorption coefficient values found for the mono- and dinuclear complexes in water.

Protonation of the Ground State. *Effect of pH on the Absorption Properties of TPAC Complexes.* Absorption measurements for each of the four TPAC complexes in the 1−14 pH range (not shown) evidence no significant changes of the spectra. The protonation occurs at much higher acidities for which the Hammett acidity function[32] H_0 has to be used.

Figure 2 shows the absorption spectra of the dinuclear compound **PP** from $H_0 = -0.4$ to $H_0 = -4.9$. This compound contains only one protonable nitrogen (belonging to the TPAC); therefore, the pK_a of the central acridine moiety of the bridging ligand can easily be determined. The spectra show the appearance of a new band at 376 nm, which is therefore attributed to the absorption of the protonated acridine moiety of the TPAC in the complex. The intensity of the MLCT band (between 400 and 500 nm) before the appearance of the new absorption feature
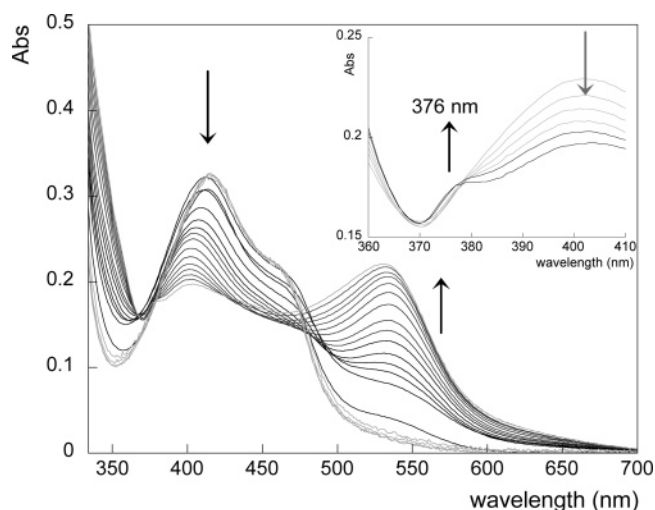
Figure 4. Absorption spectra of the MLCT transitions of [(tap)$_2$ Ru TPAC Ru (tap)$_2$]$^{4+}$ (**TT**) for increasing powers of protonation: pH 1.6, 1, 0.8 ; $H_0 = -0.6$, -1.5, -1.8, -2.2, -2.3, -2.5, -2.7, -2.9, -3.1, -3.3, -3.4, -3.6, -3.9, -4.2, -4.5, -5.2, -5.4. Inset: zoom on the 360−410 nm range of the absorption spectra, with the growth of a weak band at 376 nm attributed to the protonation of the TPAC ligand.

at 376 nm decreases slightly with a bathochromic shift of only a few nanometers. The occurrence of isosbestic points (328, 396, 469 nm) indicates the presence of two species in equilibrium. The absorption spectra of the mononuclear **P** compound (Figure 3) from $H_0 = -0.4$ to -7.9 also exhibit the appearance of a band around 376 nm and a decrease in the MLCT band as observed for the **PP** complex.

For the dinuclear compound **TT** (Figures 4 and 5), analysis of the effect of changes of pH is more complicated because of the presence of several protonable nitrogens. However, the same type of changes as those reported in the literature[33] for other tap complexes ([Ru (tap)$_3$]$^{2+}$, [Ru (tap)$_2$bpy]$^{2+}$, [Ru tap (bpy)$_2$]$^{2+}$) is observed in the absorption spectra, obviously due to protonations of tap ligands. Thus from pH 1.6 to $H_0 = -5.4$, the protonation of a tap ligand induces the growth of a new band at 530 nm, whereas the initial MLCT band decreases (Figure 4). The λ_{max} of this new band at 530 nm is not shifted in this acidity range, whereas the maximum of the initial MLCT band at 415 nm shifts slightly to the red (13 nm). As previously
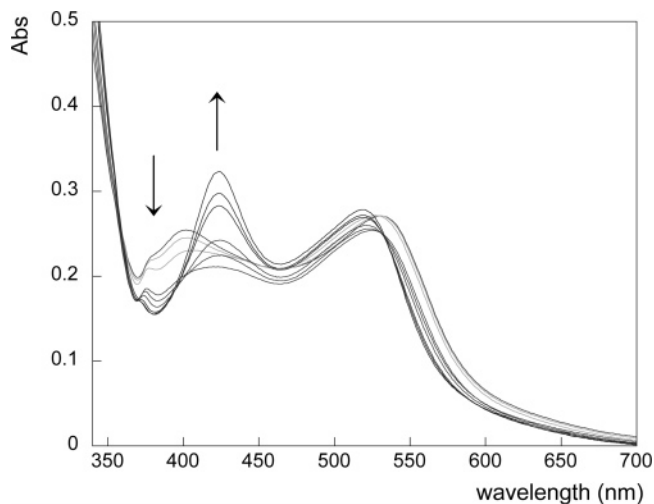
Figure 5. Absorption spectra of $[(tap)_2 Ru\ TPAC\ Ru\ (tap)_2]^{4+}$ (**TT**) for increasing powers of protonation: $H_0 = -5.4, -5.6, -5.9, -6.2, -6.5, -6.7, -7.2, -7.3, -7.4$.

reported for $[Ru\ (tap)_3]^{2+}$,[33] no clear isosbestic points are defined. Around 376 nm (Figure 4, inset), where the protonated TPAC absorbs in **PP** and **P**, a weak shoulder appears and could thus correspond to the protonation of the TPAC. By further increasing the protonating power of the solution (Figure 5), a new band appears at 423 nm and is assigned (see discussion) to other protonations of the tap ligands, whereas the 530 nm band is shifted hypsochromically (10 nm). A similar behavior is observed for the **T** complex, except for the shoulder in the 376 nm region, which seems completely hidden by the Ru-tap absorption bands (not shown).

Determination of the pK_a Values of the Ground State (Table 2). Several methods can be used to determine the pK_a values.[34-37] The spectrophotometric method already described in the literature[38-44] for other ruthenium complexes was chosen. The pK_a values for the ground state of the four TPAC complexes and reference complexes for comparison purposes obtained by spectrophotometry are collected in Table 2. They have been determined from the inflection point of the curve "absorption versus pH or H_0 (the acidity function)" at a wavelength where the largest change of the absorption is measured.

For the **PP** complex, the comparison between the so determined pK_a values, i.e., -4 (inset of Figure 2), with the pK_a value of free acridine,[45] i.e., 5.6, reveals an important effect of complexation of the TPAC ligand by the Ru(II) ions. The fact that the MLCT band is quasi not affected by protonation will be discussed later, in comparison with the data gathered for the **P** complex and the two tap analogues.

For the **P** complex, the spectrophotometric titration curve at 376 nm shows the presence of two inflection points (inset of Figure 3), corresponding to two distinct pK_a values for the TPAC ligand, the first at $H_0 = -2.9$, and the second at $H_0 = -7.2$. Indeed, one side of the TPAC ligand in **P** has a nonchelated phen motif, which in addition to the acridine moiety is of course a site of protonation. One could speculate that the sequence of pK_a in **P** would follow the sequence of pK_a of the corresponding free ligands (i.e., 5.6 for the acridine motif and 4.96 for the phen motif).[46] However, the complexation by the Ru(II) ion could influence the basicity of the acridinic and phenanthrolinic nitrogens differently. Therefore, an unambiguous attribution of the pK_a values for **P** is difficult. We could assign the first pK_a to the acridine (-2.9) and the second (-7.2) to the phen motif of complex **P** on the basis of a comparison with the data obtained with **PP**. In such a case, a pK_a of -2.9 for **P** is not

extremely less negative than -4 for **PP** in which the acridine motif is the only protonable site. It is indeed normal that the pK_a of **PP** would be more negative than the pK_a of **P** because the second complexation of TPAC probably decreases the basicity of the acridinic nitrogen and should thus induce a shift of the corresponding pK_a toward more negative values as compared to **P**. Another possible explanation would consist of assigning the first pK_a of **P** (-2.9) to the phen motif of TPAC and the second (-7.2) to the acridine. As the phen motif is located further from the Ru center than the acridine, the phen motif should be less influenced by the complexation than the acridine. In that case, the second protonation of **P**, thus localized on the acridine, should be shifted toward more negative values as compared to **PP** ($pK_{a1} = -4$ for **PP** and $pK_{a2} = -7.2$ for **P**) because of the fact that the ligand is already protonated. We will further explain that this second explanation for **P** is preferred.

In the case of the **TT** dinuclear complex (Figures 4 and 5), the absence of isosbestic points could stem from the presence of several species in equilibrium (as already observed for example with $[Ru\ (tap)_3]^{2+}$).[33] Nevertheless, the first pK_a value can be estimated (Figure 6) from the inflection point of the titration curve at 530 nm, which yields a pK_a value of -2.7, attributed to protonation of tap. This value is indeed consistent with the pK_a values of $[Ru\ (tap)_2bpy]^{2+}$ (-2.6), $[Ru\ (tap)_2phen]^{2+}$ (-2.7) and $[Ru\ (tap)_3]^{2+}$ (-3).[33] As there are eight possible protonation sites on the tap ligands in **TT**, it is of course not possible to determine all these pK_a values. The second titration curve, with an associated pK_a of -7.3 (Figure 6), could correspond to protonation of either other tap ligands or the acridine center. As the parent complex $[Ru\ (tap)_2bpy]^{2+}$ also presents an absorption band growing at 420−430 nm (cf. Figure 5 for **TT**) in the same range of H_0,[33] we propose to attribute this increasing spectral band to protonation of tap species in the **TT** complex. Concerning the acridine protonation, it is most probable that it occurs in the same range of acidity as for the phen-based complexes but is hidden by the more intense Ru-tap absorption bands (see inset of Figure 4).

For the **T** complex, the titration curve at 530 nm leads to a $pK_a = -2.7$, thus the same value as for the dinuclear complex. For more negative values of H_0 (~ -7), the absorption data did not allow the determination of another pK_a value, probably because of the presence of yet another type of protonable site as compared to **TT**, i.e., the unchelated phen nitrogens of the TPAC ligand.

For all the tap complexes studied up to now, the first protonation induces (as shown in Figure 4) an important bathochromic shift (~ 100 nanometers) due to stabilization by protonation of the π^* orbital centered on the tap ligands. Concerning the phen-based complexes **P** and **PP**, no such red shifts of the MLCT bands are observed when the protonating power is increased. This absence of shift might be attributed to the fact that the electron excited upon light absorption is more localized on the phen part close to the Ru center than on the acridine moiety of the TPAC ligand, so that the protonation of the acridine nitrogen in the ground state does not affect much the MLCT transition in absorption.

Protonation of the Excited State. *Effects of the pH on the Emission Properties of the TPAC Complexes.* The luminescence of the four TPAC complexes is strongly affected by the acidity of the aqueous solution, i.e., the intensity at the emission maximum of the basic form decreases with the acidity for the four studied complexes. A luminescence titration curve versus pH is shown in Figure 7 for the mononuclear **T** complex.
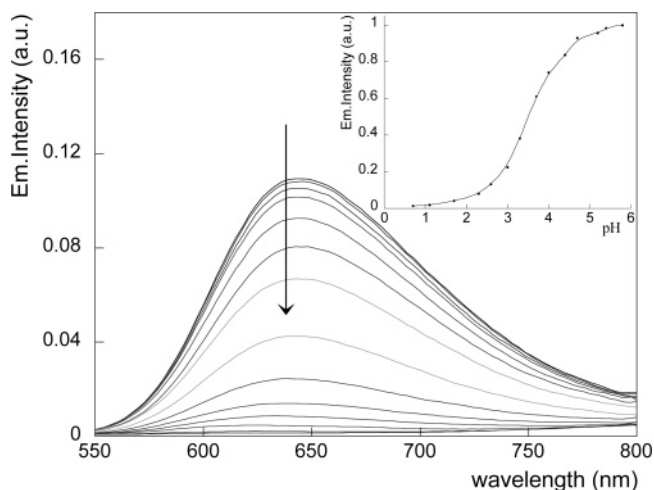
TABLE 2: Selected Wavelengths for the Absorption Titration Curves and Subsequent pK_a Values Found for the First (1) and Second (2) Protonation of the Four TPAC Complexes and a Reference Complex; the Corresponding Protonated Ligands Are Given in Italics

complex	λ_{max}^{abs} (nm)	pK_{a1}		pK_{a2}	
P	376 (1/2)	−2.9	*TPAC (phen)*	−7.2	*TPAC (acridine)*
PP	376	−4	*TPAC (acridine)*	−	−
T	415, 530	−2.7	*tap*		
TT	415, 530 (1)/423 (2)	−2.7	*tap*	−7.3	*tap*
[Ru (tap)$_2$phen]$^{2+}$	410, 465, 540	−2.7	*tap*		

TABLE 3: Wavelengths of the Maximum of Absorption in the MLCT Band and Emission of the Four TPAC Complexes and a Reference Complex (B = basic form, BH$^+$ = acid form), and Corresponding τ_B^0 under Air

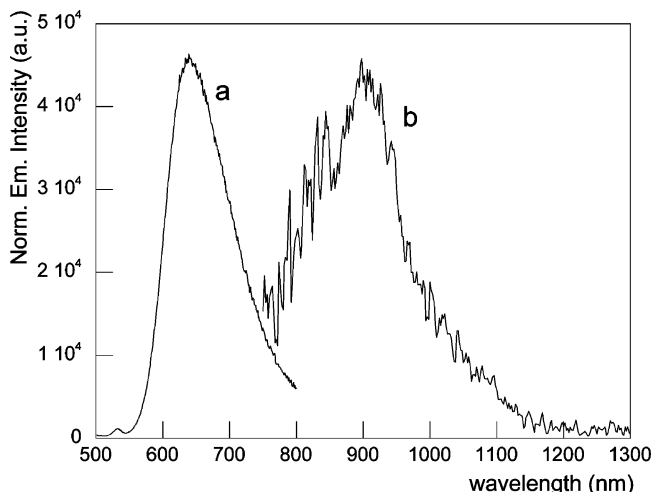| complex	λ_{max}^{abs}(B) (nm)	λ_{max}^{abs}(BH$^+$) (nm)	λ_{max}^{em}(B) (nm)	λ_{max}^{em}(BH$^+$) (nm)	τ_B^0 (ns)
P	450	469	614		500
PP	450	462	614		491
T	462	530	640	900	759
TT	465	530	640	920	739
[Ru (tap)$_2$phen]$^{2+}$	465	540	642	900	690

Interestingly, the drop of luminescence at 640 nm (Table 3) is accompanied by an emission increase at 900 nm (Table 3 and Figure 8), which is, however, too weak to perform quantitative analyses in emission intensity. Moreover, even at pH 1, when the luminescence of BH^{+*} should be at the maximum, its
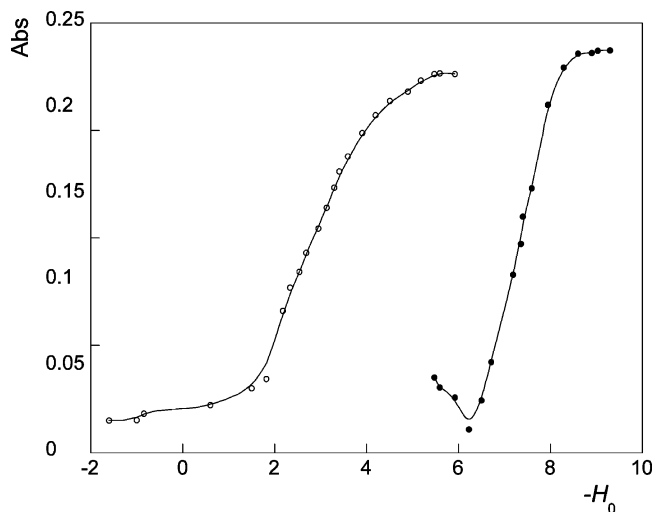

Figure 6. Absorption plotted versus -H_0 for [(tap)$_2$ Ru TPAC Ru (tap)$_2$]$^{4+}$ (**TT**) at 530 nm (○) and at 423 nm (●). Both inflection points lead to pK_a values attributed to the protonation of tap ligands.

luminescence lifetime is too short for our detection system (≤1 ns). The same type of luminescence behavior in the 640 and 900 nm region is observed for the **TT** complex. These near IR emissions are typical of protonated excited [Ru (tap)$_2$L]$^{2+}$ species as indicated by comparison with other tap complexes (Table 3 and reference 33). As in absorption, the bathochromic emission of the protonated excited-state is caused by the stabilization of the protonated tap π^* orbital. In contrast, for the **P** and **PP** compounds, although a decrease in the luminescence intensity of the basic excited form (B*) is also observed with decreasing pH, no emission is detected in the near-infrared at low pH values.

Determination of the Excited-State pK_a Values.*[47−50] For the polyazaaromatic ruthenium(II) complexes, the lowest triplet excited-state reached after excitation and relaxation corresponds to a ^{3}MLCT [Ru^{3+}−L$_2$L$^{\bullet-}$]* species with an increased electronic density on the most stabilized π^* orbital of the ligands. Therefore the basicity is generally exalted in the excited ^{3}MLCT state,[39] which leads to a change in the acid−base equilibrium from the ground to the excited state (Scheme 1).

The conditions for a thermodynamic acid−base equilibrium in the excited-state are: $k_1[H^+] > k_3$ (thus $k_1\tau_B^0[H^+] > 1$) and $k_2 > k_4$ (thus $k_2\tau_{BH^+}^0 > 1$), with τ_B^0 = lifetime of the basic form of the excited complex (non protonated form), $\tau_{BH^+}^0$ = lifetime of the acid form of the excited complex (protonated form), k_1

Figure 7. Emission spectra of [Ru (tap)$_2$TPAC]$^{2+}$ (**T**) with decreasing pH. Inset: luminescence titration curve from which the inflection point gives the apparent pK_a*.

Figure 8. Normalized emission spectra of [Ru (tap)$_2$TPAC]$^{2+}$ (**T**): (a) in neutral solution, recorded with a Hamamatsu R928 PMT detector; (b) at pH 1.6, recorded with an IR Ge-detector.

SCHEME 1: Equilibrium of the Acid−Base Couples in the Ground and Excited States

$$B^* + H^+ \underset{k_2}{\overset{k_1}{\rightleftharpoons}} BH^{+*}$$

$$h\nu \updownarrow k_3 \qquad\qquad \downarrow k_4$$

$$B + H^+ \rightleftharpoons BH^+$$
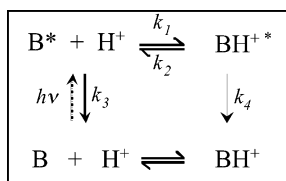
B stands for the basic form, BH$^+$ is the acid form, k_1 the rate constant of protonation, k_2 the rate constant of deprotonation in the excited state, k_3 the inverse of the excited-state lifetime τ_B^0 of B and k_4 the inverse of the excited-state lifetime $\tau_{BH^+}^0$ of BH$^+$.

= protonation rate constant in the excited state and k_2 = deprotonation rate constant of the protonated excited state.

(a) pK$_a$ from the Emission as a Function of pH.* On the basis of the kinetic Scheme 1, eq 1 is obtained under steady-state conditions

$$\frac{I_0}{I} = 1 + \frac{k_1 \tau_B^0}{(1 + k_2 \tau_{BH^+}^0)}[H^+] \tag{1}$$

in which I is the emission intensity of the basic form of the excited complex (B*) at different pH and I_0 its emission intensity in basic conditions (equilibrium completely shifted to the left). Thus, at the inflection point of the curve I versus pH (see for example inset of Figure 7) and if only B emits at the wavelength of measurement, the pH corresponds to

$$pH_{\text{inflection}} = \log \frac{k_1 \tau_B^0}{1 + k_2 \tau_{BH^+}^0} \tag{2}$$

The values determined for this pH$_{\text{inflection}}$ for the four TPAC complexes are collected in Table 4; they are higher than the pK$_a$ values of the corresponding ground states by about 5 or 6 units. This should reflect as mentioned above the much higher basicity of the excited state as compared to the ground state.

If the equilibrium is reached in the excited state (thus if $k_2 \tau_{BH^+}^0 > 1$), eq 2 becomes

$$\log \frac{k_1 \tau_B^0}{k_2 \tau_{BH^+}^0} = pK_a^* + \log \frac{\tau_B^0}{\tau_{BH^+}^0} = pH_{\text{inflection}} = pK_{a_{\text{apparent}}}^* \tag{3}$$

Consequently the pK$_a$* value can be determined from eq 3, i.e., from the pH values at the inflection point, called also pK$_{a_{\text{apparent}}}^*$, if as mentioned above, the equilibrium is established in the excited state. This condition is fulfilled when $k_2 \tau_{BH^+}^0 > 1$. Actually we have no access to $\tau_{BH^+}^0$ because protonated **P** and **PP** do not emit in aqueous solution and their excited-state lifetimes cannot be measured by transient absorption spectroscopy in a nanosecond timescale. It is the same problem for the transient emission or absorption for **T** and **TT**. The fact that the lifetimes of BH^{+*} would be much shorter than one nanosecond has an important consequence. This would mean that maybe the acid−base equilibrium is not reached in the excited state because of the too short lifetime of BH^{+*}, so that as mentioned above, eq 3 would no longer be valid and the true pK$_a$* value could not be determined. If this is the case and if at the other extreme, $k_2 \tau_{BH^+}^0$ can be neglected versus 1, eq 2 transforms into eq 1′, which corresponds to a Stern−Volmer relation.

$$\frac{I_0}{I} = 1 + k_1 \tau_B^0 [H^+] \tag{1'}$$

In such a case, the luminescence decays of B* under pulsed excitation should correspond to single-exponential signals, and the same Stern−Volmer relation as eq 1′ with the same slope should be obtained by plotting τ_0/τ versus the protons concentration. This is indeed the case, as shown in Figure 9 and by the data of Table 4, in which the rate constant k_1 has been calculated from the Stern−Volmer relation in emission intensities and lifetimes. The high value of the protonation rate constant for excited **P** (1.5×10^{10} s^{-1}) as compared to that of **PP**, **T**, and **TT** could be due to the fact that in that case the protonation site is the unchelated phen moiety of the TPAC ligand. This site is far away from the metal ion with two protonable nitrogen atoms without steric hindrance by aromatic rings, in contrast to the TPAC acridine nitrogen. Such a protonation site is of course not present in complex **PP**, where the proton has to be located on the acridinic nitrogen of the bridging TPAC ligand (Figure 1). These conclusions are in agreement with our second hypothesis for the attribution of the pK$_a$ values determined above in the ground state for **P**, i.e., the first pK$_a$ corresponding to the protonation of the phen motif of TPAC and the second to the acridine moiety. For **T** and **TT**, the rate constants k_1 correspond of course to the protonation of the tap ligands.

(b) Förster's Cycle. The acidity constants K_a* of the excited molecules can also be estimated from a method known as "Förster's cycle".[51,52] If ΔH and ΔH^* correspond respectively to the enthalpies of the protonation reaction in the ground and excited state and if ΔE_B^{00} and $\Delta E_{BH^+}^{00}$ are the differences in energy between the ground and excited states of B and BH$^+$ (Figure 10), eq 4 can be written

$$\Delta H^0 - \Delta H^{0*} = \Delta E_{BH^+}^{00} - \Delta E_B^{00} \tag{4}$$

If it is assumed that the entropies of reaction are the same in the ground and excited states, then

$$\Delta G^0 - \Delta G^{0*} = \Delta E_{BH^+}^{00} - \Delta E_B^{00} \tag{5}$$

or another expression equivalent to eq 5 can be written

$$pK_a^*(F) = pK_{a_{\text{ground}}} + \frac{0.625}{T}(\tilde{\nu}_B - \tilde{\nu}_{BH^+}) \tag{6}$$

in which pK$_{a_{\text{ground}}}$ stands for the pK$_a$ in the ground state, T is the temperature (K), $\tilde{\nu}_{B/BH^+}$ the wavenumbers (cm^{-1}) related to the 0−0 electronic transitions of the basic form (B) and acid form (BH$^+$) of the complex and pK$_a$* (F) is called Förster's pK$_a$. Equation 6 allows thus a determination of the difference of pK$_a$ (or difference of ΔG^0, Figure 10) between the ground and excited-state reactions, without taking into account the fact that the equilibrium is or is not reached during the lifetimes of the excited states. These pK$_a$*(F) values present the advantage of being comparable within a series of similar compounds, such as for example the tap complexes for which the errors associated with the different approximations (i.e., ΔS constant) are in the same order of magnitude. Some authors in the literature have calculated ΔG^{0*} or pK$_a$* from the absorption spectra.[53] In this work, however, we did not perform those calculations because it has been well-established that the singlet−triplet intersystem crossing process takes place within ~100 fs,[54] so that protonation of the ^{1}MLCT state for a reasonable pH domain could never compete with the intersystem crossing. Thus we have calculated the pK$_a$*(F) values from the emission data only (Table

TABLE 4: Values of pH at the Inflection Point (pH$_{inflection}$) of the Four TPAC Complexes and a Reference Complex from the Luminescence Titration Curves of the Basic Form of the Complexes; Quenching Rate Constant k_1 Calculated from the Slope of I_0/I and τ_0/τ versus [H$^+$]; Values of the Förster's pK_a's (pK_a*(F)) from Eq 6 (by Using the Franck−Condon Emission Data to Determine $\tilde{\nu}_B$ and $\tilde{\nu}_{BH^+}$)

complex	pH$_{inflection}$	k_1 (M^{-1} s^{-1}) from I_0/I[a]	k_1 (M^{-1} s^{-1}) from τ_0/τ[b]	pK_a*(F) from FC$_{em}$
P	3.9	1.5×10^{10}	1.9×10^{10c}	−
PP	1.5	1.9×10^7	2.0×10^7	−
T	3.5	3.2×10^9	3.6×10^9	6.5
TT	3.5	5.4×10^9	4.7×10^9	7.2
[Ru (tap)$_2$phen]$^{2+}$	3.3	3.2×10^9	3.8×10^9	6.4

[a] Errors estimated to ∼5%. [b] Errors estimated to ∼10%. [c] **P** needs several purifications by preparative thin layer chromatography[28] in order to get rid of **PP** present in trace amounts in the sample.
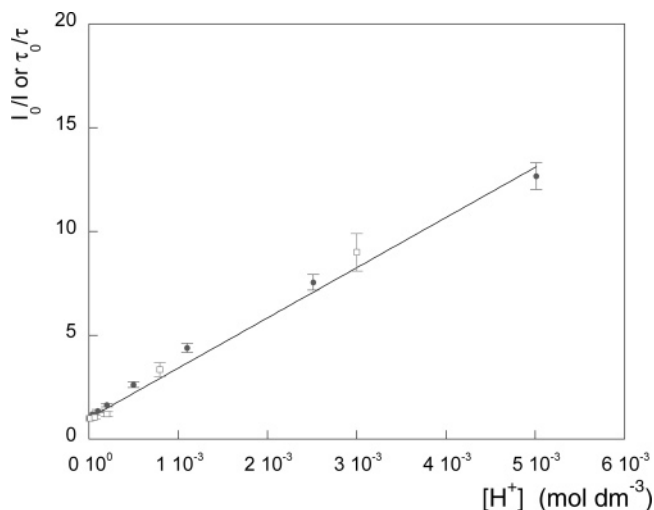
Figure 9. Stern−Volmer plot obtained by plotting I_0/I (●) and τ_0/τ (□) versus [H$^+$] for [Ru (tap)$_2$TPAC]$^{2+}$ (**T**) under air at 614 nm.
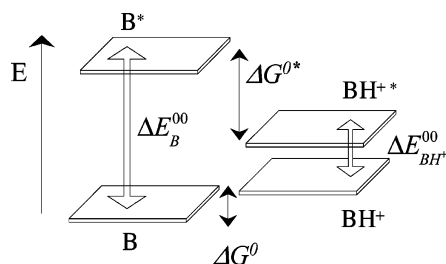
Figure 10. Schematic diagram: energy levels for the basic form in the ground (B) and excited state (B*) and for the protonated form in the ground (BH$^+$) and the excited state (BH^{+*}) with the associated energies for the 0−0 transition (ΔE_B^{00} and $\Delta E_{BH^+}^{00}$), and the free energy of the protonation reaction in the ground (ΔG^0) and the excited state (ΔG^{0*}).

4).[55] The Förster's pK_a* for **P** and **PP** could not be determined because the luminescence of the corresponding BH^{+*} species could not be detected, in contrast to the tap complexes. The data of Table 4 indicate that the Forster's pK_a* values are the same for the mononuclear tap complexes of the present and previous study.[33] However, for [Ru(tap)$_3$]$^{2+}$, the pK_a*(F) was lower (pK_a*(F) = 5)[33] because of the presence of three π-deficient tap ligands instead of two. Moreover, for complex **TT**, for which a tap ligand is nevertheless also protonated, the pK_a*(F) value is higher (7.2). This difference could be attributed to differences of entropy factors between the dinuclear complex and the series of mononuclear tap complexes for which the entropy factors could be considered as similar but probably different from those of the dinuclear species.

Comparison of the Effect of pH on the Absorption and Emission Processes. It is clear from this work, in contrast to dppz complexes such as [Ru(bpy/phen)$_2$dppz]$^{2+}$ that do not emit

in water,[23,56] that the TPAC complexes with either phen or tap ancillary ligands are all luminescent in water. This allows a comparison of the pH effect on the absorption and emission processes. In absorption for an acidic medium, there is a sharp difference between the TPAC complexes depending on the ancillary ligands, tap or phen. When the ground state is protonated on the tap ligand, an important bathochromic effect is observed on the MLCT band of the absorption spectrum. Thus in the Franck−Condon state reached by this MLCT excitation, the promoted electron is localized on the tap π* orbital stabilized by protonation of the nitrogen atoms. The relaxation process leads to a protonated ^{3}MLCT state, whose luminescence is shifted bathochromically compared to that of the excited basic ^{3}MLCT state. In contrast for the MLCT absorption of the protonated **P** and **PP** complexes, only a very weak bathochromic effect on the MLCT band due to protonation of the ground state is observed. This could be due to the fact that by MLCT excitation, in the Franck−Condon state, the electron would be promoted on the chelated phen part of the TPAC ligand and would not move further. In contrast, after relaxation to the ^{3}MLCT, the situation would be different because the excited electron would be localized on the acridine moiety (for **PP**) or on the unchelated phen part (for **P**) of the TPAC ligand, i.e., where the protonation occurs. This protonated ^{3}MLCT state is not luminescent, in contrast to the ^{3}MLCT Ru-tap.

Finally, the fact that the **T**, **TT**, **P**, and **PP** complexes can be very easily protonated in their ^{3}MLCT state should be extended to the case of the excited complexes in interaction with DNA because the DNA microenvironment is slightly more acidic (pH 4.5−5)[57,58] than the aqueous solution. Consequently, in pulsed laser experiments of systems composed of these complexes interacting with DNA, among the different possible transients that could be formed, the protonation of the excited state should be considered.

References and Notes

(1) Nakabayashi, Y.; Iwamoto, N.; Inada, H.; Yamauchi, O. *Chem. Lett.* **2006**, *35*, 722.

(2) Kirsch-De Mesmaeker, A.; Lecomte, J.-P.; Kelly, J. M. Photoreactions of Metal Complexes with DNA, Especially Those Involving Primary Photo-Electron Transfer. In *Topics in Current Chemistry*; Springer-Verlag: Berlin, 1996; Vol. 177, pp 25.

(3) Naing, K.; Takahashi, M.; Taniguchi, M.; Yamagishi, A. *Inorg. Chem.* **1995**, *34*, 350.

(4) Erkkila, K. E.; Odom, D. T.; Barton, J. K. *Chem. Rev.* **1999**, *99*, 2777.

(5) Metcalfe, C.; Thomas, J. A. *Chem. Soc. Rev.* **2003**, *32*, 215.

(6) Pierard, F.; Kirsch-De Mesmaeker, A. *Inorg. Chem. Commun.* **2006**, *9*, 111.

(7) Elias, B.; Kirsch-De Mesmaeker, A. *Coord. Chem. Rev.* **2006**, *250*, 1627.

(8) Vos, J. G.; Kelly, J. M. *Dalton Trans.* **2006**, 4869.

(9) Sjodin, M.; Styring, S.; Wolpher, H.; Xu, Y. H.; Sun, L. C.; Hammarstrom, L. *J. Am. Chem. Soc.* **2005**, *127*, 3855.

(10) Lomoth, R.; Magnuson, A.; Sjodin, M.; Huang, P.; Styring, S.; Hammarstrom, L. *Photosynth. Res.* **2006**, *87*, 25.

(11) Wagenknecht, H. A.; Stemp, E. D. A.; Barton, J. K. *J. Am. Chem. Soc.* **2000**, *122*, 1.

(12) Copeland, K. D.; Lueras, A. M. K.; Stemp, E. D. A.; Barton, J. K. *Biochemistry* **2002**, *41*, 12785.

(13) Karidi, K.; Garoufis, A.; Hadjiliadis, N.; Reedijk, J. *Dalton Trans.* **2005**, 728.

(14) Moucheron, C.; Kirsch-De Mesmaeker, A.; Kelly, J. M. *J. Photochem. Photobiol., B* **1997**, *40*, 91.

(15) Blasius, R.; Moucheron, C.; Kirsch-De Mesmaeker, A. *Eur. J. Inorg. Chem.* **2004**, 3971.

(16) Blasius, R.; Nierengarten, H.; Luhmer, M.; Constant, J.-F.; Defrancq, E.; Dumy, P.; van Dorsselaer, A.; Moucheron, C.; Kirsch-De Mesmaeker, A. *Chem.—Eur. J.* **2005**, *11*, 1507.

(17) Gicquel, E.; Boisdenghien, A.; Defrancq, E.; Moucheron, C.; Kirsch-De Mesmaeker, A. *Chem. Commun.* **2004**, 2764.

(18) Bijeire, L.; Elias, B.; Souchard, J. P.; Gicquel, E.; Moucheron, C.; Kirsch-De Mesmaeker, A.; Vicendo, P. *Biochemistry* **2006**, *45*, 6160.

(19) Lecomte, J.-P.; Kirsch-De Mesmaeker, A.; Kelly, J. M.; Tossi, A. B.; Görner, H. *Photochem. Photobiol.* **1992**, *55*, 681.

(20) Coates, C. G.; Callaghan, P.; McGarvey, J. J.; Kelly, J. M.; Jacquet, L.; Kirsch-De Mesmaeker, A. *J. Mol. Struct.* **2001**, *598*, 15.

(21) Elias, B.; Creely, C.; Doorley, G. W.; Feeney, M. M.; Moucheron, C.; Kirsch-De Mesmaeker A.; Dyer, J.; Grills, D. C.; George, M. W.; Matousek, P.; Parker, A. W.; Towrie, M.; Kelly, J. M. *Chem.-Eur. J.* **2007**, in press.

(22) Chambron, J. C.; Sauvage, J. P.; Amouyal, E.; Koffi, P. *Nouveau J. Chim.* **1985**, *9*, 527.

(23) Olson, E. J. C.; Hu, D.; Hörmann, A.; Jonkman, A. M.; Arkin, M. R.; Stemp, E. D. A.; Barton, J. K.; Barbara, P. F. *J. Am. Chem. Soc.* **1997**, *119*, 11458.

(24) Önfelt, B.; Olofsson, J.; Lincoln, P.; Nordén, B. *J. Phys. Chem. A* **2003**, *107*, 1000.

(25) Turro, C.; Bossmann, S. H.; Jenkins, Y.; Barton, J. K.; Turro, N. J. *J. Am. Chem. Soc.* **1995**, *117*, 9026.

(26) Olofsson, J.; Önfelt, B.; Lincoln, P. *J. Phys. Chem. A* **2004**, *108*, 4391.

(27) Brennaman, M. K.; Meyer, T. J.; Papanikolas, J. M. *J. Phys. Chem. A* **2004**, *108*, 9938.

(28) Elias, B.; Herman, L.; Moucheron, C.; Kirsch-De Mesmaeker, A. *Inorg. Chem.* **2007**, *46*, 4979.

(29) Lin, C. T.; Bottcher, W.; Chou, M.; Creutz, C.; Sutin, N. *J. Am. Chem. Soc.* **1976**, *98*, 6536.

(30) Hergueta-Bravo, A.; Jimenez-Hernandez, M. E.; Montero, F.; Oliveros, E.; Orellana, G. *J. Phys. Chem. B* **2002**, *106*, 4010.

(31) Ortmans, I.; Elias, B.; Kelly, J. M.; Moucheron, C.; Kirsch-De Mesmaeker, A. *Dalton Trans.* **2004**, 668.

(32) Rochester, C. H. *Organic Chemistry, A Series of Monographs*; Academic Press: New York, 1970; Vol. 7.

(33) Kirsch-De Mesmaeker, A.; Jacquet, L.; Nasielski, J. *Inorg. Chem.* **1988**, *27*, 4451.

(34) Jia, Z. J.; Ramstad, T.; Zhong, M. *Electrophoresis* **2001**, *22*, 1112.

(35) de Tacconi, N. R.; Lezna, R. O.; Konduri, R.; Ongeri, F.; Rajeshwar, K.; MacDonnell, F. M. *Chem.—Eur. J.* **2005**, *11*, 4327.

(36) Brown, T. N.; Mora-Diez, N. *J. Phys. Chem. B* **2006**, *110*, 20546.

(37) Knobloch, B.; Sigel, H.; Okruszek, A.; Sigel, R. K. O. *Org. Biomol. Chem.* **2006**, *4*, 1085.

(38) Giordano, P. J.; Bock, C. R.; Wrighton, M. S. *J. Am. Chem. Soc.* **1978**, *100*, 6960.

(39) Crutchley, R. J.; Kress, N.; Lever, A. B. P. *J. Am. Chem. Soc.* **1983**, *105*, 1170.

(40) De Buyl, F.; Kirsch-De Mesmaeker, A.; Tossi, A.; Kelly, J. M. *J. Photochem. Photobiol., A* **1991**, *60*, 27.

(41) Zheng, G. Y.; Wang, Y.; Rillema, D. P. *Inorg. Chem.* **1996**, *35*, 7118.

(42) Rugge, A.; Clark, C. D.; Hoffman, M. Z.; Rillema, D. P. *Inorg. Chim. Acta* **1998**, *279*, 200.

(43) Liu, F. R.; Wang, K. Z.; Bai, G. Y.; Zhang, Y. G.; Gao, L. H. *Inorg. Chem.* **2004**, *43*, 1799.

(44) O'Donoghue, K.; Penedo, J. C.; Kelly, J. M.; Kruger, P. E. *Dalton Trans.* **2005**, 1123.

(45) Neta, P. *J. Phys. Chem.* **1979**, *83*, 3096.

(46) McBryde, W. A. E.; Brisbin, D. A.; Irving, H. *J. Chem. Soc.* **1962**, 5245.

(47) Vander Donckt, E. *Progress in Reaction Kinetics*; Porter, G., Ed.; Pergamon Press: Oxford, U.K., 1970; Vol. 5.

(48) Vander Donckt, E. *Eléments de Photochimie Avancée*; Pierre Courtot-Herman: Paris, 1972.

(49) Ireland, J. F.; Wyatt, P. A. H. *Adv. Phys. Org. Chem.* 1972; Vol. 12.

(50) Mulder, W. H. *J. Photochem. Photobiol., A* **2003**, *161*, 21.

(51) Förster, T. *Z. Elektrochem.* **1950**, *54*, 32.

(52) Weller, A. *Z. Elektrochem.* **1952**, *56*, 662.

(53) Thompson, A.; Smailes, M. C. C.; Jeffery, J. C.; Ward, M. D. *J. Chem. Soc., Dalton Trans.* **1997**, 737.

(54) Yoon, S.; Kukura, P.; Stuart, C. M.; Mathies, R. A. *Mol. Phys.* **2006**, *104*, 1275.

(55) It is known that determination of the 0−0 electronic transition raises some problems for the Ru(II) complexes because the absorption corresponds to a S_0−S_1 transition, whereas the emission originates from an excited state that has mixed character between the singlet and triplet characteristics, referred to as the ^{3}MLCT (T_1) state. Without the vibrational structure of the spectrum, an exact value for the 0−0 transition in emission is not easily obtained. We made the approximation that it corresponds to the Franck−Condon energy in emission (from λ_{max} emission). The emission profile I_{em}-(λ) has been transformed into $I_{em}(\tilde{\nu})$. This transformation has been performed by using the following equation: $I_{em}(\lambda) \propto \partial Q/\partial \lambda \rightarrow I_{em}(\tilde{\nu}) \propto \partial Q/\partial \lambda \ \partial \lambda/\partial E \propto \partial Q/\partial \tilde{\lambda} \ \lambda^2$ (where Q is the total number of photons).

(56) Friedman, A. E.; Chambron, J.-C.; Sauvage, J.-P.; Turro, N. J.; Barton, J. K. *J. Am. Chem. Soc.* **1990**, *112*, 4960.

(57) Lamm, G.; Pack, G. R. *Proc. Natl. Acad. Sci. U.S.A.* **1990**, *87*, 9033.

(58) Pack, G. R.; Wong, L. *Chem. Phys.* **1996**, *204*, 279.